Fiber Optic Capillary Sensor with Smart Optode for Rapid Testing of the Quality of Diesel and Biodiesel Fuel

Michal Borecki, Piotr Doroz, Przemysław Prus, Paweł Pszczółkowski, Jan Szmidt
Warsaw University of Technology
Institute of Microelectronics and Optoelectronics
Warsaw, Poland
E-mail: borecki@imio.pw.edu.pl

Jarosław Frydrych
Automotive Industry Institute
Warsaw, Poland.
e-mail: j.frydrych@pimot.eu

Michael L. Korwin-Pawlowski
Département d'informatique et d'ingénierie
Université du Québec en Outaouais
Gatineau, Québec, Canada
e-mail: michael.korwin-pawlowski@uqo.ca

Andrzej Kociubiński, Mariusz Duk
Lublin University of Technology
Department of Electronics
Lublin, Poland.
e-mail: akociub@semiconductor.pl

***Abstract*—There are many fuel quality standards introduced by national organizations and fuel producers. Usual techniques for measuring the quality of fuel, as for example cetane index, fraction composition and flash point, require relatively complex and expensive laboratory equipment. Therefore, testing of fuel is not rapid and can be costly. On the fuel user side, fast and low cost sensing of useful state of biodiesel fuel is important. One of the devices that address this task is the fiber optic capillary sensor in which forced local conversion of diesel fuel into vapor is implemented. The present paper concentrates on the critical elements the construction of the sensor as well as on the interpretation of experimental results. We have investigated the construction of the micro heater and the technology of smart capillary optrode preparation. We propose a capillary optrode construction and technology that reduces unwanted light coupling, as well as a new micro heater construction that uses a silicon carbide heating element. Our experimental assumption is that diesel fuel quality can be correlated with the type and concentration of its bio-components. We examined fuels that are mixtures prepared from components that are in line with European Union standards. The components used are petrodiesel fuel and bio-esters as well as edible rapeseed oil. For the mentioned fuels, we showed that the results of experiments are easy to interpret and that the useful state of diesel and biodiesel fuels can be determined from the time of local heating that is required for vapor phase creation and the local time of vapor bubble formation.**

Keywords-biodiesel fuel; fuel quality; useful state of fuel; fiber optic capillaries; fiber optic sensors; capillary sensor; smart capillary optrode

I. INTRODUCTION

This paper's focus is on selected aspects of construction of sensor that uses capillary optrode and enables rapid testing of quality of diesel and biodiesel fuels, the principle and preliminary results of which were presented in [1].

A. Diesel and biodiesel fuel production examination and usage

Rudolf Diesel constructed the first internal combustion engine using pure plant oil as carburant in 1912. The fuel was 100% peanuts oil; therefore, today this fuel classification is PPO – pure plant oil. The next time engines operated on PPO were built in 1985 [2].

Classical fuels are made from distillated products of crude oil. After distillation the oil composition depends on the process and on the crude oil parameters. The parameters of oil distillation process are not merely the boiling temperature but include such distillation characteristics as: initial distillation temperature (about 170ºC), end distillation temperature (about 370ºC) and the fractional contents temperatures. Those characteristics determine also the basic fuel parameters.

On the practical side, diesel engine performance, fuel consumption, and emitted pollutants result from the combustion process. The environment of combustion, the injected fuel's form and the fuel quality all play a primary role in the diesel combustion process. One of the most important diesel fuel quality parameters is ignition quality. The ignition quality depends on the molecular composition of the fuel. The ignition quality in turn is linked with ignition delay time, which is the time between the start of injection and the start of combustion. Measurements of ignition quality of fuel (CN) have to be carried out in the Cooperative Fuel Research (CFR -5) engine, under carefully controlled test conditions. The smaller is the delay of testing, the CN value is greater. The CN scale is based on the characteristics of know chemical single components liquid hydrocarbons. Therefore, the CFR-5 engine is also called cetane engine. The basic disadvantage of such approximation to fuel quality measurement is the high cost of the measurement device and the complexity of the procedure. The alternative approximation is the use of ignition quality tester (IQT™)

and the ASTM D6890/EN 15195(IP 498) test methods. The mentioned devices can be seen in [3, 4].

Nowadays, producers define the useful state of diesel fuel by several parameters: cetane number (min 51.0), density (860 to 890 kg/m^3), and distillation temperatures (for example T_{90} maximal value is 360°C), kinematic viscosity at 40°C (3.5 to 5.0 mm^2/s), etc. Other diesel fuel parameters characterize its operability: carbon residue, water and sediment, cloud point, conductivity at 20°C, oxidation stability, acidity, copper corrosion, flashpoint, lubricity, appearance, and color [5]. For the ordinary fuel user such collection of parameters is often too complex for practical use because their testing requires special laboratory equipment. Therefore, fuel examination is not rapid and can be costly.

The introduction of biodiesel fuel increases the number of parameters connected with the bio-component content [6]. In this situation the user requires the simplest possible answer to a question: Is that fuel useful for my engine?

B. *Economical reason of sensor of diesel and biodiesel fuel examination*

Sensing of useful state of biodiesel fuel is exceptionally important for car fleet owners and farmers.

Car fleet owners are interested because of legal regulations and of the risks of buying poor quality fuel [7]. In certain countries, including Poland, units of public administration, production and customers the law prescribes public auction for transactions of larger quantities of fuel. In such auction the ordered fuel is certified on the day of delivery as meeting national standards, like the Polish norm PN-EN 590. The purchased quantity of the fuel is often split between different tanks belonging to the buyers. During the fuel transfer into the buyers' tanks the buyers' representative may be present. Even though the ordered fuels may have to a certificate of quality, the buyers often reserve the rights to check the quality of the fuel. Quite often the delivered fuel quality tests are at the option of the buyers, and are often waived because of the associated costs, with sometimes conflicts arising when the poor quality is discovered at a later stage.

Farmers are often very interested in examination of diesel fuel quality because they can produce bio-fuel components for their own use. The characteristics of those home-produced components are not optima [8]. One can see clear differences between the freshly pressed technical rapeseed oil and the edible rapeseed oil, which is chemically clarified and stabilized with antioxidants, such as vitamin E. For practical fuel application the technical rapeseed oils have too small cetane numbers and too high viscosities. It seems that one of the reasons of low biodiesel fuel mixtures usage by farmers is the absence of a low cost device to evaluate its useful state [9]. In certain regions, there are in use mixtures of rapeseed oil with diesel fuel, sometimes they are modified with n-butanol or ethanol [10]. However, the viscosities of oils decrease with the increase of temperature. For these reasons, in tropical countries the potential of using biodiesel fuels is larger. The uses of mixtures of soapnut oil with petrodiesel fuel are discussed in [11]. It turns out that, despite significant differences in fuel viscosity and flash point, the observed engine parameters with the prepared mixtures were very similar [12].

In a European study, it was observed that using the biodiesel fuel of the first generation at low environment temperatures can lead to the degeneration of engine parameters [13]. Therefore, production standards for biodiesel fuel were introduced: density at 15°C (ISO3675) and temperature of fluidity for the transitional periods of season and winter (DIN EN 116). The disadvantages of biodiesel fuel can be overcome by fuel processing [14] or by using biopetrodiesel fuel mixtures [15]. There are also publications describing low energy processes for upgrading the technical parameters of biofuels. For example: transestrification of soybean oil with the use microwave and nanopowders enables creation of biodiesel fuel, which meets the requirements of the EN-14214 norm [16]. A new generation of 100% biodiesel fuel can be made with isomerization [17, 18]. Neste Oil proposes NExBTL bio component that can be used as 100% biodiesel fuel that means the diesel fuel without petrodiesel components, and is known as NesteGreen 100. The hydrogenated vegetable oils (HVO) are also used as biodiesel components. Their advantage is agreement with diesel particulate filter (DPF) of engines.

C. *Critical points of diesel fuel conversion into energy*

The starting point of this development of a new sensing method of the useful state of diesel and biodiesel fuels was to consider the two critical points of fuel conversion into energy. The first is the injector of atomized fuel into the combustion chamber by forcibly pumping it through a small nozzle. The second critical point is the exhaust of gases filtered with the diesel particulate filter. Periodically, the DPF has to be taken up to high temperatures to burn off the matter it has collected, which is realized by contact of DPF with a part of fuel vapor [19].

Typically, fuel is injected into the cylinders just after the vapor fires and the exhaust valve opens. At injection point, the fuel vaporizes and a part of vapor moves down the exhaust to the DPF and cleans it in a precisely controlled injection scheme [20]. Because biodiesel fuel has a higher distillation temperature than petrodiesel fuel, it does not vaporize as fast [21, 22]. Some of the biodiesel fuel can end up adhering to the injector, the cylinder wall or runs past the rings, diluting the engine oil and diluting DPF deposits instead of cleaning it.

Therefore, the examination of vapor creation parameters of biodiesel fuels is critical to evaluate its useful state regardless of the composition of fuel. The methods of spray forming observation in diesel engine have been used [23], but are not good for integration into a sensor device.

In this work, we present new developments and new applications of on capillary photonic sensors working on the principle of monitoring optical intensity changes in dynamically forced measurement cycles, first postulated in [24]. We present the idea of the sensor, the construction of the head, the experimental results of testing biodiesel fuels for their quality for use, and conclusions.

The sensors use fiber optic capillaries in which the phase of the filling liquid changes locally to gas when forced by local heating, while the propagation of light in the capillary is monitored. Therefore, the sensors examine simultaneously many parameters of the liquids. To evaluate the performance of the sensors, we used oils with known quality.

II. IDEA OF SENSOR HEAD

The sensor head idea is inspired by one of most critical diesel engine element that is fuel injector and nozzle. The actual dimensions of the typical nozzle showed in Fig. 1 are ID/Id = 4, L/Id = 5 and Id = 0.2mm. The fuel injector nozzle diameters depending on construction can vary from 50 to 200µm [25].

The influence of relation between nozzle dimensions, pressure ratio on the type of diesel fuel flown is under investigations [26]. The character of the fuel flow through the nozzle depends strongly on the pressure difference. It can be classified as cavitating or non-cavitating type, while in the non-cavitating flow case we distinguish between the turbulent and the laminar flow. The caviting flows happen when the difference in pressures is high enough. The input pressure (P_i) can vary from 15MPa to 110MPa. The output pressure (P_n) is of the order of 6MPa.

Typical temperatures inside the fuel injection nozzle are from 235 to 275°C, the maximum does not exceed 300°C [25]. The flame temperatures in the cylinders (T_n) are about 1500°C and the wall temperatures are under 350°C. Therefore, we cannot replicate the flame temperatures and pressures in small portable sensor devices.

On the other hand, the volume of a single injection of the fuel is at the range of 3÷50mm^3. The fuel injected into cylinder forms a spray and enters the cylinder in about few milliseconds [28]. Then it vaporizes and flames.

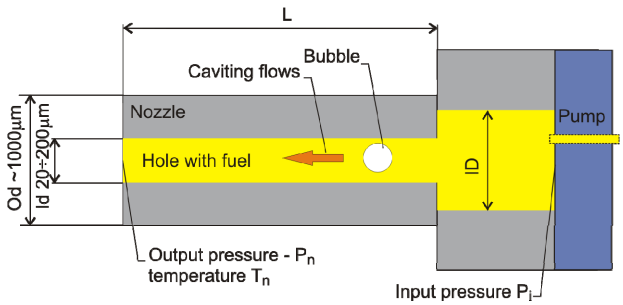

Figure 1. Schematic construction of the nozzle.

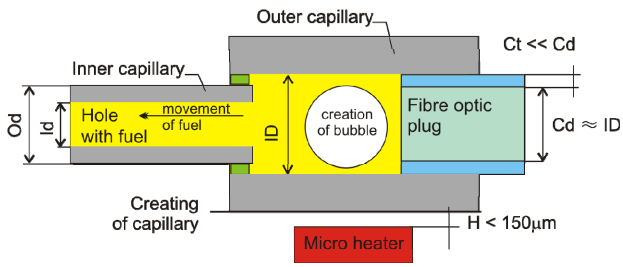

Figure 2. Schematic construction of sensor head.

These processes are correlated with the quality of ignition, which forms one of the major factors of the fuel quality. The second factor when considering biodiesel fuel is connected with fuel viscosity. Therefore, we intend to examine in our sensor the fuel vaporization and forced flow in conditions that are as close to reality as possible. We have to create a setup allowing the examination of partial evaporation of fuel, which take place in the nozzle and can move the fuel into the orifice of few hundreds micrometers diameter. Such a nozzle can be modeled with two glass capillaries that would allow observation of the direct optical fuel phases and their movement. The capillary with the smaller outer diameter can be positioned inside the bigger capillary using glue forming a single-use replaceable optrode [1].

The inner temperature that is needed to create the bubble of vapor can be achieved with a local heater positioned near the capillary. With one end of capillary closed, the local heater can act as a fuel pump by producing a vapor pressure (see Fig. 2). The set of commercially available capillaries produced by VitroCom enables to prepare the optrode that is characterized by dimensions close to those of practical nozzles. For example; as the inner capillary we can use CV3040Q capillary that Id = 300µm as the outer capillary we can use CV7087Q capillary, which ID = 700µm. Both capillaries can work in temperatures up to the quartz glass annealing point, which is 1070ºC. The outer capillary (CV7087Q) length should be greater than 7.8mm to move 3mm^2 of fuel.

The creation and movement of the bubble in the liquid depends on the liquid thermo-dynamical parameters as well as its viscosity and its vapor phase parameters, and also on the container's geometry and the outer thermo-dynamical conditions [29]. The faster is the bubble creation from liquid phase, the more probable is the turbulent flow of fuel in the nozzle. Therefore, we have to distinguish two stages of the bubble creation: the time of liquid fuel heating and the time of phase change from liquid to vapor that forms the bubble filling the full cross section of the capillary.

III. HEAD CONSTRUCTION

The sensor's head consists of two functional blocks: the base and the optrode [30]. The base is used to integrate the micro heater, the optical path of source and receiver as well as for positioning the optrode. The optrode is the replaceable part of the head that imitates the geometry and the main physical characteristics of a fuel nozzle and enables monitoring of creation of the vapor bubble.

A. Micro heater

The micro heater has to supply sufficient heat for the biodiesel fuel to reach over 200°C inside the capillary. We examined experimentally and by numerical modeling the map of temperatures in the model of nozzle. We used the Coventor software, a R300 NEC thermo-vision camera, and the InfReC analyzer software. The results of micro heater simulation are presented in Fig. 3.

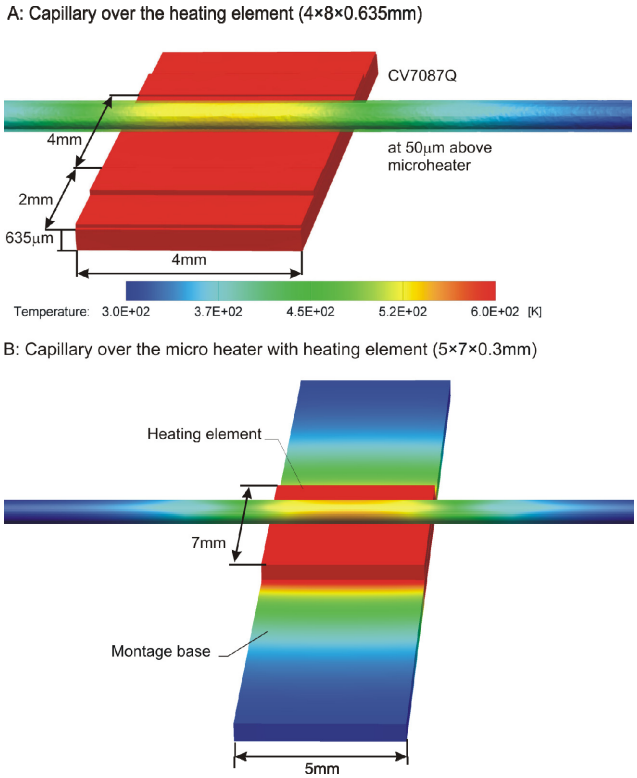

Figure 3. Temperature map in [°K] at 30s of heating for a glass capillary CV7087Q filled with diesel fuel.

In both cases, the capillary optrode and its position over heating element is the same. The situation in Fig. 3a concerns thick film type planar heating element with total dimension 4mm×8mm×0.635mm. The element is equipped with a resistance heating element and with connection pads. The resistance element area covers 4×4mm and is positioned at 50μm under the capillary. For dissipating 5W in 30 seconds the temperature of the surface of the heater reached 327°C while the temperature inside the capillary reached 247°C. The full microheater assembly (Fig. 3b) including the mounting base requires dissipating of 7W in 30 seconds to achieve the same temperature inside the capillary.

Sequential simulations showed that for the 290ºC temperature inside the filled up capillary and for the assumed distance between the capillary and micro heater surface, the micro heater with dimensions of 5mm×5mm, the upper surface temperature has to be at least 350°C. This temperature is more than can withstand the planar resistors, e.g., Vishay High Power Thin Film Wraparound Chip Resistor in type 2512 package [31]. Wire heaters can easily work at such temperatures, but since such constructions do not provide a constant and repeatable distance between the microheater and the capillary, they cannot replace the planar structures. The most favorable shape of planar microheaters is rectangular with side length from 2mm to 5mm, and the recommended power of heating is 7÷10W. The power density can reach 1.6W/mm^2, which is also too high for commercial hybrid resistors. For the heater current supply the recommended value of resistance is between 10÷50Ω. Even current dividers from Vishay like the Current Sensing Bondable Chip Resistors type S.C. are not optimal for such application. More over, the head construction requires that the microheater has to be positioned on a rectangle shaped substrate with the length of 3cm and width of 5mm. On this substrate the electrical contacts for the heating element and wire connections have to be provided, as well as isolating pads for mounting the head. The isolating regions are necessary because the head base is made of metal. The micro heater base is outlined in Fig. 4.

We have built different versions of planar micro heaters. In all construction we used alundum ceramic bases with the thickness of 635μm. For preparing the heating elements we used thick film and thin film hybrid technologies as well as monolithic silicon carbide semiconductor technologies.

The thick film technology enabled us to make a fully integrated micro heater in the form of one piece. In our investigation this element worked repeatable in 20 seconds cycle without long term resistance changes when end temperatures did not exceed 200°C. The parameters of the micro heater were stable for temperature shocks from 30°C to 200°C – the reversible resistance changes were low, within 1.5Ω at 30Ω of nominal resistance. When the temperature exceeded 200ºC we observed cracking of the resistive layer followed by the splitting of ceramic base into two parts. Therefore, we examined the two other technologies.

We used thin film metal deposition technology to prepare standalone resistance elements. The metal was deposited on a silicon substrate. There were three areas in the element: one square resistive heating area and two areas for electrical connections. The connections between the heating element and the microheater base were made by wire bonding or with high temperature conductive glue use. To bond it, we at first positioned the element on the base with dielectric glue. At that, we observed two unwanted phenomena, both due to the high temperature of the connected elements. For wire bonding technology we observed at 150°C that standard dielectric glue gave smoke, but we did not detect any rapid changes of the resistance of the micro heater. With conductive glue technology use at 300°C we observed that the high temperature connecting glue, which was specified as working up to 400°C also gave smoke while the connections resistance increased from 1 Ω to 10Ω. This increase had an unstable character, but the glue still properly positioned heating element on the base.

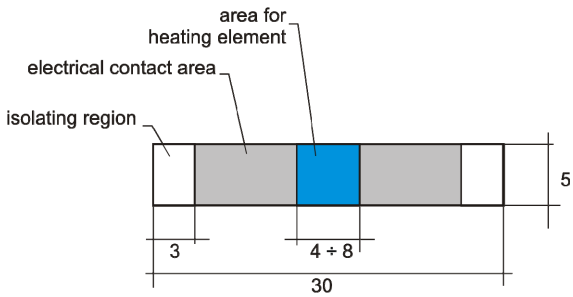

Figure 4. Micro heater base outline.

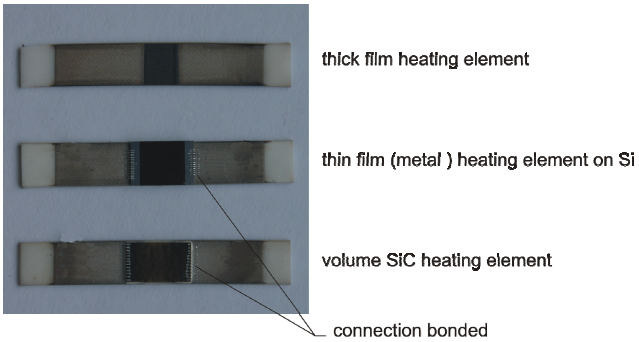

Figure 5. Tested micro heaters.

Moreover, the thin film heating element increased its resistance during heating cycles in such way that the initial resistance of following heating cycle was bigger than in previous one. We think that special passivation of thin metal layer will solve this problem.

At last we evaluated monolithic silicon carbide heating elements. The element enabled heating capillary to the required temperature in 30 second cycles. The increase of time of heating from 25 to 30 second with decreased power but maintained final temperature resulted in partial degradation of the glue used for bonding. We used high temperature conductive glue; therefore, we observed the mentioned degradation as small permanent changes in the microheater's resistance. Hence, we limited heating time to 25 seconds. The next heating cycle with maximum power was safe, when the heater was allowed to cool down to room temperature. In normal condition it required about 2 minutes for cooling. The tested micro heaters are shown in Fig. 5.

B. Path of optical signal

The creation of the bubble can be observed from outside or inside of capillary with the use of optical fibers [32]. The bubble position can vary in the area of local heating due to variation of fuel composition and real geometrical dimensions of capillaries within with their specified tolerances. Moreover, the outside observations of effects happening inside the capillary are sensitive to outer capillary cleanness [33, 34]. Therefore, the observation from outside is not optimal for measuring the bubble creation time. Observation of the bubble creation with two fibers positioned inside the capillary is not convenient for a replaceable optrode setup, and also complicates the fuel flow. To overcome those problems, we used a modified capillary optrode with a phosphor layer to convert radiation (see Fig. 6).

In the presented optrode, the phosphor converts the light from 460nm wavelength of the high power light emitting diodes, to 562nm. Only part of the light radiated in the full angle extent propagates in the inner capillary to the area of examination. The fragment of optrode where phosphor is deposited is presented in Fig. 7. When we illuminated the phosphor with the radiation of 460nm at the cross section of outer capillary of optrode we registered the presence of radiation at 460nm and 562nm wavelengths (see Fig. 8).

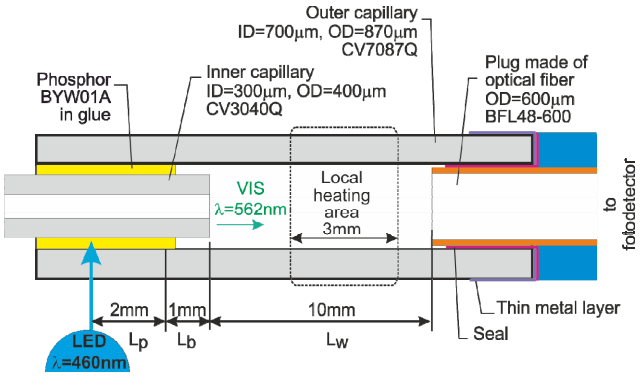

Figure 6. Optrode that uses phosphor to convert outer radiation into light inside capillary.

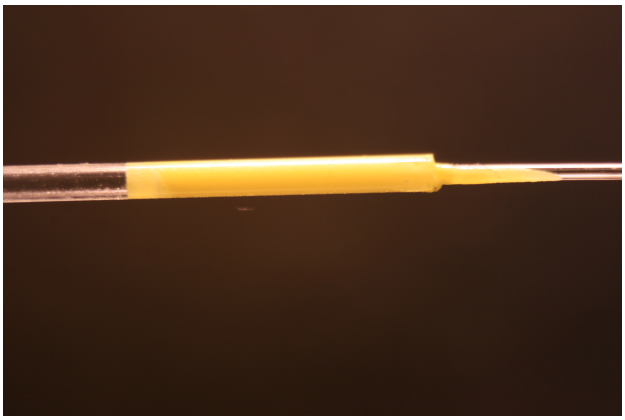

Figure 7. Optrode part where UV phosphor is deposited.

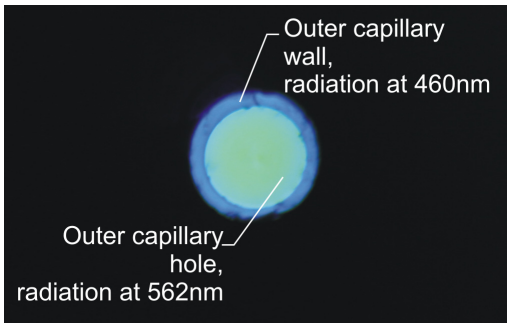

Figure 8. Cross section of outer oprtode when phosphor is radiated with radiation at 460nm wavelength, the output power is at the rank of 300nW.

To eliminate the coupling to the receiver of the unwanted radiation propagating into the wall of outer capillary, we used two means of protections. First, the receiver fiber plug was inserted into optrode. Second, the optrode walls at the plug side were covered with a thin metal layer (see Fig. 9) [35]. The optical quality of thin film protection is presented in Fig. 10, where the optical beam coupled into the outer capillary has 2mW of power at 675nm. No optical signal that would output from the capillary walls is in evidence, contrary to the situation presented in Fig. 8.

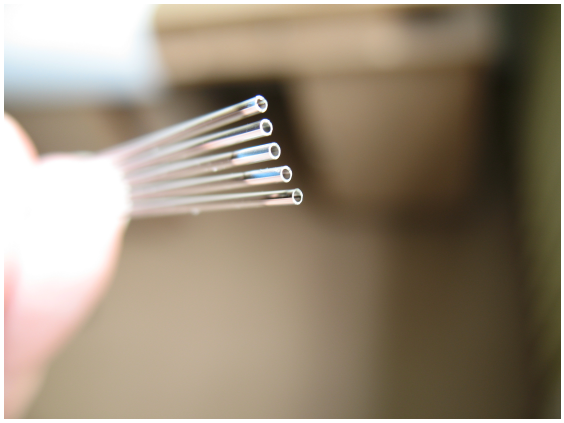

Figure 9. The end of optrodes with deposited thin film metal layers.

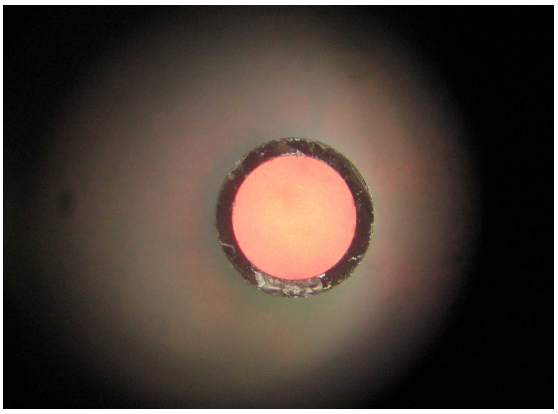

Figure 10. The end walls of outer capillary protected with metal layer, when 2mW optical beam was coupled into the capillary.

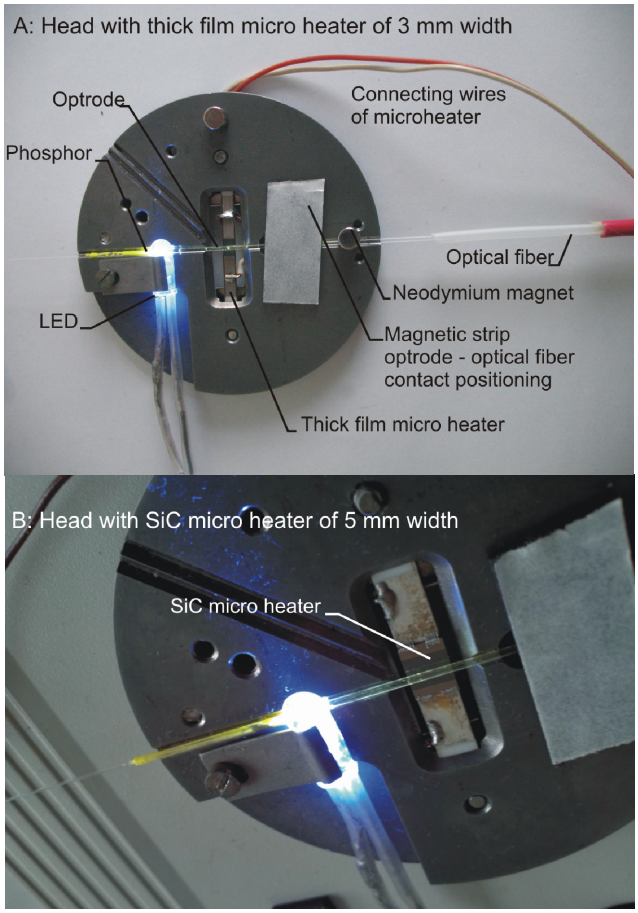

Figure 11. The head construction.

The efficiency of light conversion in the developed optrode is low, but acceptable. We optimized the optrode elements position: Lp, Lb and Lw (see Fig. 6), as well as the method and parameters of phosphor deposition. After optimizing the construction, we got from a L7113QBC-G LED operating at 20mW, at the end of the plug made from optical fiber, 111nW for an empty capillary and 0.3µW for a capillary filled with biodiesel fuel. The uncertainty of low signal level in our construction was 10nW. The optrode was held in position with elastic magnetic strips, while the optical fiber was secured with miniature neodymium magnets. The construction of the head is presented in Fig. 11. The two types of micro heaters were installed. In Fig. 11A, the holders of micro heater are better visible than in Fig. 11B. The electrical connections from micro heater to power supply are made at some distance from the heating element to secure their proper working temperature.

Though we predicted that thick film micro heater may be not proper for biodiesel fuel examinations, we checked such a possibility by making a series of fuel examination experiments. The results showed that a critical degradation of such micro heater happens after over a dozen measuring cycles. Therefore, for further experiments we used only micro heaters with SiC heating element.

C. *Optoelectronic signal processing*

As the light source driver we built an electronic device that enabled current modulation from DC to 50 kHz at selected frequencies, which was equipped with configurable current limiters to prevent accidental LED burning. To improve the rejection of ambient light influence on the experimental results in our experiment we used electrically modulated light with 1kHz frequency.

The optoelectronic detection unit of our own construction had an SMA fiber input and consisted of an integrated photo-amplifier and a band-pass filter with amplification and RMS detection. We used the S8745-01, AD8253, UAF42, AD536 and AD8250 components. In the realized construction we were able to measure signals in the range from 10nW up to 500nW with 2nW accuracy when the signal duration was 0.01s. The optoelectronic unit was connected to a personal computer through an analog input IOtech personal Daq 3000 16bit/1MHz USB data acquisition system. We fed the heater from a laboratory power supply Hameg HM8143 controlled by the analog output from Daq. The view of sensor hardware set-up is presented in Fig. 12. We also used a Daq 3000 system to monitor the temperatures of the measuring head base and of the surrounding ambient with two LM35DT circuits connected by low pass filters.

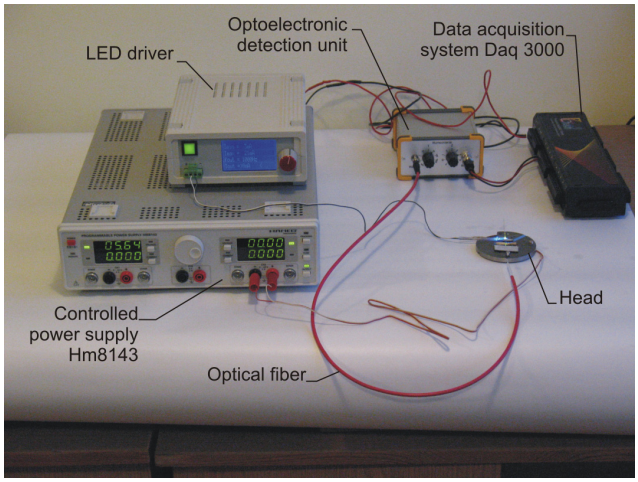

Figure 12. View of experimental set-up, [1].

To operate the system, we designed a script in DASYLab with a 0.01s sampling rate. The script automates the measurements and automatically switched off the micro heater when the light signal dropped under a specified value corresponding to the point of vapor bubble creation or when maximum time of local heating is exceed. The length of signal registration was 60s.

IV. EXPERIMENTAL RESULTS

In this section are presented the experimental procedure and the results of examination of different diesel and biodiesel fuels.

A. Experiment procedure

At the start of the experiment the optrode was closed with a fiber optic plug without use of sealant and then is placed in the head. The LED was switched on at the power of 20mW. The initial output signal was measured and when it was greater than 110nW we assumed that the optrode was qualified to use (see Fig. 13). Next, the optrode was filled with fuel, after which its end was closed with fiber optic plug secured with sealant. When there were bubbles of gas observed at the initial state of experiment, the optrode and capillary had to be withdrawn [29]. When the capillaries were filled uniformly by the liquid, the optrode was placed into the head and the initial levels of transmitted signal were examined and used as reference levels. In normal situation the signal should be greater than 300nW. We normalized such initial signal level to 4 a.u. (in Fig. 13).

As the examined fuel in the useful state was semitransparent, we expected initially high signal levels, and then low signal levels when the bubble would appear. The bubble directed the signal from the liquid to the capillary walls [32]. When the transmitted signal decreased rapidly it gave the impulse to switch off the microheater. We terminated the heating when the signal dropped under 2.5 a.u.

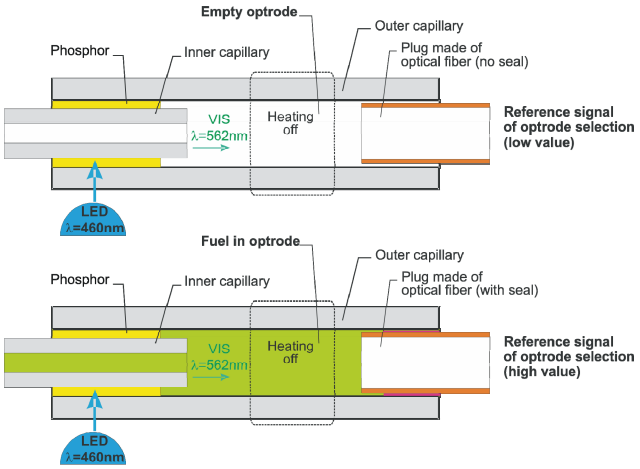

Figure 13. Initial situations of experimental procedure.

Depending on the thermo-dynamical conditions; the vapor gas phase moved the fuel to the open end with a laminar or a turbid flow. The turbid flow could be detected optically after the experiment as a presence of series of small bubbles in the optrode. Depending on the flow type and fuel decomposition after heating we could observe two situations presented in Fig. 14.

Both situations presented in Fig. 14 result in the reduction of the output optical signal and are difficult to be distinguished in the measurement, but are easy to be distinguished visually. The small bubble appears at the stable position over center of micro heater, where the temperature achieves its maximum. We thought that a small bubble appeared and lasted in the fuel due to structural changes induced by heating to some components that were added after distillation, or to some decomposition of bio-components, since the bubble was particularly present after examination of edible oils [36].

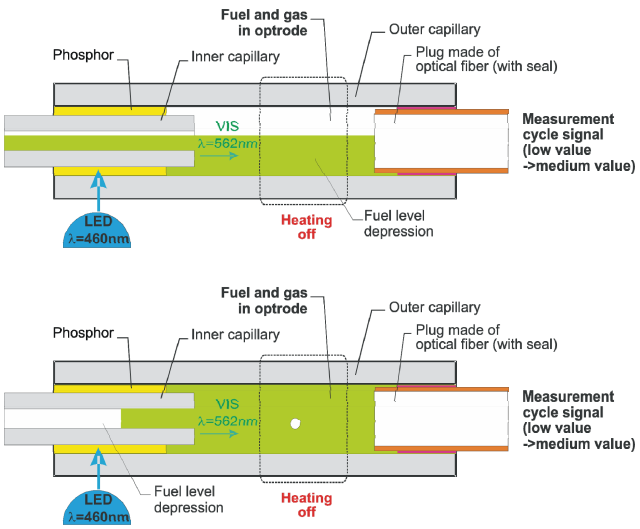

Figure 14. Two possible situations after local heating procedure.

B. Diesel and biodiesel fuels used for examination

We examined six potential fuels in which set five fuels were prepared from the same pure and fresh components at different ratios. For these fuels we use petrodiesel, fatty acids methyl esters (FAME) and additives according to EU standard. As sixth potential fuel we suppose edible rapeseed oil (ERO). The edible rapeseed oil has to be distinguished from technical rapeseed oil (TRO). Technical rapeseed oil is the direct product of rapeseed corn pressing, while edible oil is the product of technical oil purification and addition of antioxidants.

We defined the fuel quality as: premium, good, acceptable for selected engines and acceptable for special engines. As the premium quality fuel we evaluated the clear and fresh petrodiesel component that was mixed with selected additives according to EU standards. The good quality fuel was premium quality fuel mixture with 10 of FAME. The acceptable for selected (tolerant) engines fuels consisted of 30 and 60% of FAME. We assumed that the FAME with additives fuel known as 100% biodiesel fuel could be used in special engines.

Selected parameters of prepared fuels are grouped in Table I. The examination of the fuels in the laboratory prior to the experiment showed that fuels P100, B10, B30 and B60 were meeting the norms. The FAME fuel starts to distillate at an unacceptable high temperature. B100 - modified FAME may start distillation at T0 = 280ºC while T10≈T50≈T90≈340ºC, therefore, its usage in classic diesel engines is questionable [13]. The used ERO is characterized by a very quick start of distillation at 170-200ºC, then no observable change to 295ºC, where it starts distillate as fuel up to 363ºC. The B100, TRO and ERO did not meet the distillation standards of fuels.

TABLE I. SELECTED PARAMETERS OF PREPARED FUELS

Parameter	Fuel acronym				
	P100	B10	B30	B60	B100
Assumed fuel quality	P	G	Ab	Ab	Bb
Base oil [%]	100	90	70	40	0
FAME [%]	0	10	30	60	100
Density at 15ºC [kg/m^3]	832.6	837.4	847.0	862.3	883.2
Temp of flame [°C]	74	75.5	79.5	90	163
Kinematic viscosity at 40ºC [mm^2/s]	3.367	3.432	3.595	3.934	4.509
CI	54.9	57.7	57.5	56.8	*
CN	59.6	57.3	54.9	54.0	51.2
T_0 [ºC]	188.6	195.6	196.7	200.2	369*#
T_{10} [ºC]	225.7	230.4	242.1	278.1	*
T_{90} [ºC]	345.5	343.6	344.1	345.3	*

Abbreviations used: FAME – Fatty acids methyl esters (bio-component); CI – cetane index, CN – cetane number, T0 temperature of distillation start, T_X – temperature of x% volume of distillation, * - our lab equipment do to allow of such examination, value given in [14]. Assumed fuel quality set: P – premium, G – good fuel, Ab – acceptable bio fuel for selected engines, Bb – acceptable biofuel for special engines.

C. Examination of biodiesel fuels using the developed sensor

Our aim was to distinguish fuels by their quality. For this purpose we set in the experiment the power of micro heater and the maximum time of local heating. The 5W of power in thick film heating element and corresponding 7W of power dissipated in SiC micro heater in up to 25 seconds enabled to produce vapor phase for fuels that meets the norm as well as ERO.

We examined at least 3 times samples of each fuel, and on the following figures we present representative measurement cycle signal. As micro heater we used the SiC component.

We made the first experiments with P100 fuel at two powers of heating 5W and 7W (Fig. 15 and Fig. 16). The experiments showed that increasing the power from 5W to 7W reduced the average time of heating τ from 14.5 seconds to 9 seconds, and it reduced the average time of vapor phase creation Δτ from 0.2 seconds for 5W, to 0.1 seconds for 7W. The reductions in those times were in agreement with the theory of thermo dynamics.

The next experiments were made with 7W heating power and their results are presented in Fig. 17 to Fig. 20.

From our experimental results we saw that P100, B10 and B30 fuels did not differ significantly. The B60 fuel formed in our heating condition a vapor phase, but the mixture was characterized by very high dispersion of time of heating - τ.

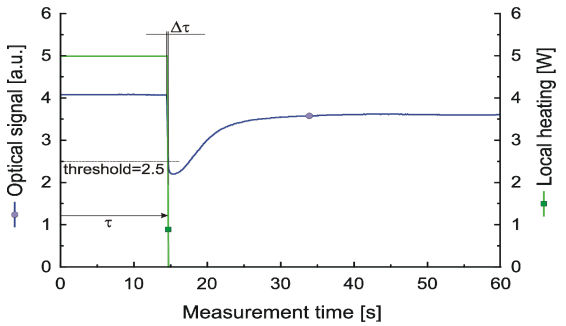

Figure 15. Measurement procedure representative signal of P100 heated with 5W.

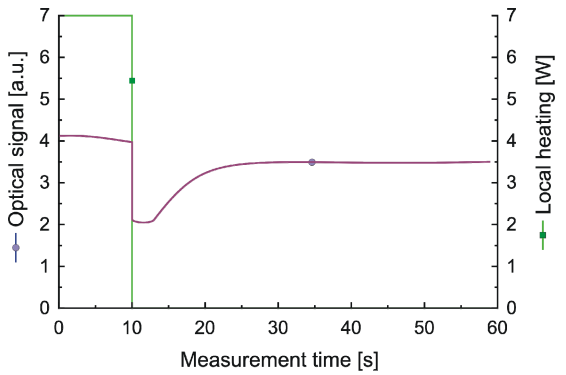

Figure 16. Measurement procedure signals of P100 heated with 7W.

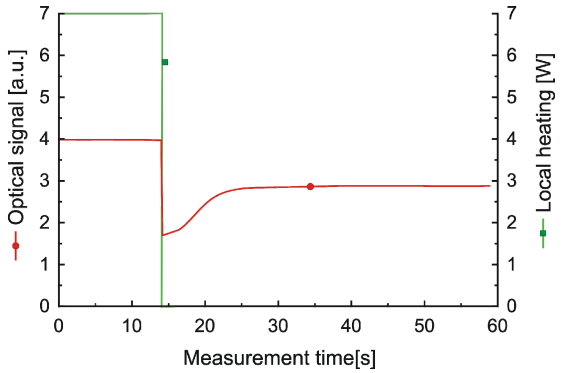

Figure 17. Measurement procedure signals of B10 heated with 7W.

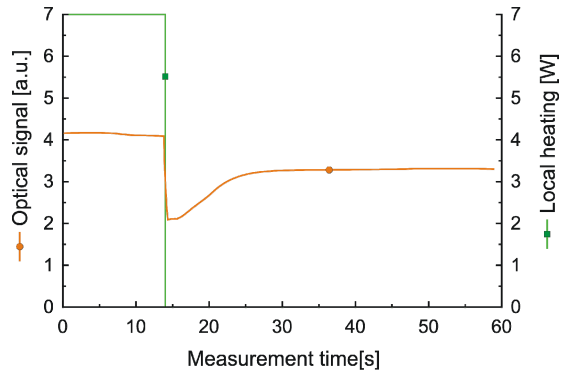

Figure 18. Measurement procedure signals of B30 heated with 7W.

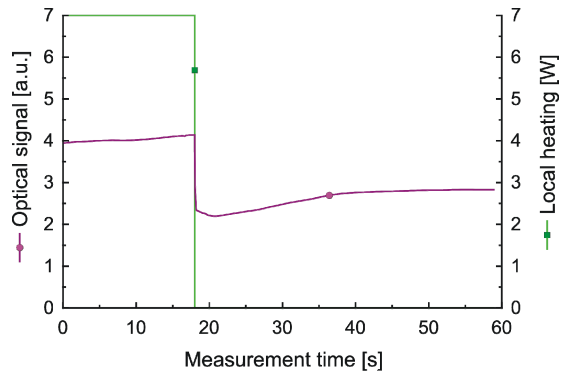

Figure 19. Measurement procedure signals of B60 heated with 7W.

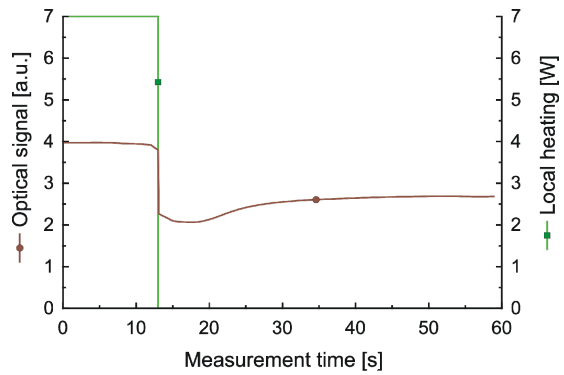

Figure 20. Measurement procedure signals of ERO heated with 7W.

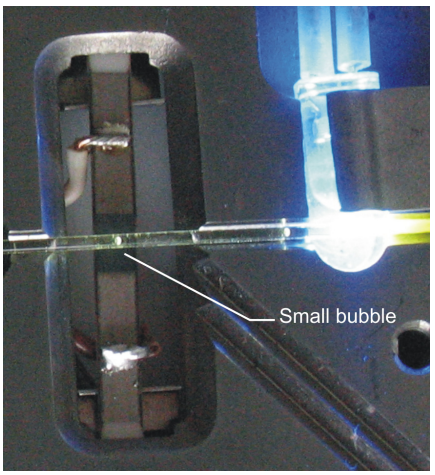

Figure 21. Small bubble remaining after heating of rapeseed edible oil in the center of the micro heater.

B100 required a longer time of heating to form bubble phase than our procedure enables. Only 30% of samples showed bubble creation in 25 seconds of local heating. This was made intentionally to enable proper classification of diesel fuel with acceptable parameters while time of heating is considered as a one of key factors. Sometimes B100 showed a lower time of bubble creation than ERO. Interestingly, according to our experimental data the B100 seemed to be a worse fuel than ERO. The ERO forms vapor phase in all cycles was similar to that of B10 fuel. But ERO had the lowest τ dispersion, which was in agreement with its distillation starting point at 170-200ºC. This is not a good property for a fuel. For ERO we observed a repeatable presence of a small bubble that remained after heating of edible rapeseed oil in the center of the micro heater (see Fig. 21).

We think that was the result of thermal decomposition of rapeseed edible oil components. It was most probably connected to the degradation of vitamin E, which occurs at 200ºC. Therefore, in ERO we examined only a part of distillation parameters, but this disadvantage could be corrected by observation of optrode after sample examination.

The summarized results of experiment of fuel examination are presented in Table II. What was expected but not obvious, our head was not sensitive to local heater construction as long as the temperature conditions of heating were the same. We see an agreement of the results collected with hybrid micro heater presented in [1] and those presented in this paper measured using the SiC micro heater.

TABLE II. EXAMINED PARAMETERS OF FUELS HEATED WITH 6W

Parameter	Fuel acronym					
	P100	B10	B30	B60	B100	ERO
Average τ [s]	9	12	13	22	*	13
Average Δτ [s]	0.10	0.13	0.18	0.30	*	0.64
Percent of samples with created bubble	100	100	100	100	30	100

*- the average value does not exist.

On the base of data collected in the experiments we can set the parameters determining the useful state of biodiesel fuel as: the upper limits of average time of heating – avg(τ), the range of dispersion of time of heating – std(τ) and the upper limit of time of vapor phase creation – max(Δτ). The analysis of data showed that in our method the useful state of diesel biodiesel fuel was directly and firmly connected with the gas phase creation. For example, the unacceptable fuels are characterized by Δτ greater than 0.3s while premium fuels Δτ have to be lower than 0.13s.

CONCLUSIONS

We proposed a sensor working on the principle optical examination of fuel under local heating. Our optoelectronic devices allowed conducting the experiment in ambient room conditions. The analysis of the measured signals of diesel and biodiesel fuels showed the relationship of times of gas phase creation parameters with the useful state of diesel fuel. We showed that the information on useful state of diesel fuel could be presented in the form of recommended ranges and times of fuel heating and vapor creation. Because the heating was taking place in a closed capillary, the fuel did not ignite during experiments. We conclude that the proposed construction may be in future the base of commercially marketable instruments.

The future work will consist of optimization of the construction especially enabling observation of optrode above the center of micro heater. The sensor construction needs to be integrated into a complete portable instrument and be built more resistant for use in harsh environments outside of the laboratory. For this purpose, the first step was achieved, as thanks to indirect light coupling the optrode walls are not much sensitive to soiling. The next required step is the development of new simpler in usage optrode plug.

ACKNOWLEDGMENT

This work was supported by: the European Union structural funds grant InTechFun task 5, “Multi parametric classificatory of liquid biofuels useful state”.

REFERENCES

[1] M. Borecki, P. Doroz, J. Szmidt, M.L. Korwin-Pawlowski, A. Kociubiński, and M. Duk, “Sensing method and fiber optic capillary sensor for testing the quality of biodiesel fuel,” IARIA, Proc. Sensordevices 2013, pp. 19–24.

[2] G. Knothe, “Historical perspectives on vegetable oil-based diesel fuels,” Industrial Oils, vol. 12, 2001.

[3] http://www.compass-instruments.com/waukesha.shtml, accessed 05.12.2013

[4] http://www.aet.ca/index.php?section=20, accessed 05.12.2013

[5] Department of Industry, Science and Resources, “Setting national fuel quality standards - Discussion paper 4,” in “Operability fuel parameters (petrol and diesel),” Environment Australia, 2001.

[6] D. Mueller, M.F. Ferrão, L. Marder, A.B. da Costa, and R. de Cássia de Souza Schneider, “Fourier transform infrared spectroscopy (FTIR) and multivariate analysis for identification of different vegetable oils used in biodiesel production,” Sensors, vol. 13, 2013, pp. 4258–4271.

[7] G. Mothé, M. Castro, M. Sthel, G. Lima, L. Brasil, L. Campos, A. Rocha, and H. Vargas, “Detection of greenhouse gas precursors from diesel engines using electrochemical and photoacoustic sensors,” Sensors, vol. 10, 2010, pp. 9726–9741.

[8] N. Li, Q. Zhou, X. Li, W. Chu, J. Adkins, and J. Zheng, “Electrochemical detection of free glycerol in biodiesel using electrodes with single gold particles in highly ordered SiO_2 cavities,” Sensors and Actuators B: Chemical, vol. 196, 2014, pp. 314–320.

[9] P.L. Faccendini, M.É. Ribone, and C.M. Lagier, “Selective application of two rapid, low-cost electrochemical methods to quantify glycerol according to the sample nature,” Sensors and Actuators B: Chemical, vol. 193, 2014, pp. 142–148.

[10] I. Barabas, A. Todorut, and D. Baldean, “Performance and emission characteristics of an CI engine fueled with diesel-biodiesel-bioethanol blends,” Fuel, vol. 89, 2010, pp. 3827–3832.

[11] R.D. Misra and M.S. Murthy, “Performance, emission and combustion evaluation of soapnut oil–diesel blends in a compression ignition engine,” Fuel, vol. 90, 2011, pp. 2514–2518.

[12] C. Ketlogetswe and J. Gandure, “Blending cooking oil biodiesel with petroleum diesel: a comparative performance test on a variable ic engine,” Smart Grid and Renewable Energy, vol. 2, 2011, pp. 165–168.

[13] M. Balat and H. Balat, “A critical review of biodiesel as a vehicular fuel,” Energy Convers Manag., vol. 49, 2008, pp. 2727–2741.

[14] S. Gryglewicz, “Rapeseed oil methyl esters preparation using heterogeneous catalysts,” Bioresource Technology, vol. 70, 1999, pp. 249–253.

[15] A.R. Sadrolhosseini et al., “Physical properties of normal grade biodiesel and winter grade biodiesel,” Int. J. Mol. Sci., vol. 11, 2011, pp. 2100–2111.

[16] W. Gis, A. Zoltowski, and A. Bochenska, “Properties of the rapeseed oil methyl esters and comparing them with the diesel oil properties,” J. of KONES Powertrain and Transport, vol. 18, 2011, pp. 121–127.

[17] N.E. Leadbetter et al., “Fast, easy preparation of biodiesel using microwave heating,” Energy & Fuels, vol. 20, 2006, pp. 2281–2283.

[18] M.C. Hsiao, C.C. Lin, and Y.H. Chang, “Microwave irradiation-assisted transesterification of soybean oil to bio-diesel catalyzed by nanopowder calcium oxide,” Fuel, vol. 90, 2011, pp. 1963–1967.

[19] M.V. Twigg and P.R. Phillips, “Cleaning the air we breathe – controlling diesel particulate emissions from passenger cars,” Platinum Metals Rev., vol. 53, 2009, pp. 27–34.

[20] B. Kegl, “Numerical analysis of injection characteristics using biodiesel fuel,” Fuel, vol. 85, 2006, pp. 2377–2387.

[21] M. Gumus, C. Sayin, and M. Canakci, “The impact of fuel injection pressure on the exhaust emissions of a direct injection diesel engine fueled with biodiesel–diesel fuel blends,” Fuel, vol. 95, 2012, pp. 486–494.

[22] W. Yuan, A.C. Hansen, and Q. Zhang, “Vapor pressure and normal boiling point predictions for pure methyl esters and biodiesel fuels,” Fuel, vol 84, 2005, pp. 943–950.

[23] B. Kegl, M. Kegl, and S. Pehan, “Optimization of a fuel injection system for diesel and biodiesel usage,” Energy & Fuels, vol. 22, 2008, pp. 1046–1054.

[24] M. Borecki, M. L. Korwin-Pawlowski, and M. Bebłowska, “A method of examination of liquids by neural network analysis of reflectometric and transmission time domain data

from optical capillaries and fibers," IEEE J. Sensors, vol. 8, 2008, pp. 1208–1213.

[25] D.L. Siebers and L.M. Pickett, "Injection pressure and oritice diameter effects on soot in DI diesel fuel jets," in Thermo- and fluid dynamic process in diesel engines 2 - Selected papers from Diesel 2002 conference Valencia, Spain, J.H. Whitelaw, F. Payri, C. Arcoumanis, and J-M. Desantes, Eds., Springer-Verlag, Berlin, Heidelberg, New York, 2002, pp. 109–131.

[26] X. Wang and WH. Su, "A numerical study of cavitating flows in high-pressure diesel injection nozzle holes using a two-fluid model," Chinese Sci Bull, vol. 54, 2009, pp. 1655–1662.

[27] N. Ladommatos, Z. Xiao, and H. Zhao, "The effect of piston bowl temperature on diesel exhaust emissions," Proc. IMechE. vol. 219 Part D: J. Automobile Engineering, 2005, pp. 371–388.

[28] C. Crua, J.C. Evans, D.A. Kennaird, and M.R. Heikal, "In-cylinder study of the formation, autoignition and soot production of diesel sprays at elevated pressures," 9th International Conference on Liquid Atomization and Spray Systems (ICLASS) Sorrento, Italy, 13-17 July 2003, http://eprints.brighton.ac.uk/2184/ access 07.02.2014

[29] M. Borecki, M. Korwin Pawlowski, P. Wrzosek, and J. Szmidt, "Capillaries as the components of photonic sensor micro-systems," J. of Mater. Sci. and Technol., vol. 19, 2008, pp. 065202.

[30] M. Borecki, M.L. Korwin-Pawlowski, M. Beblowska, J. Szmidt, and A. Jakubowski, "Optoelectronic capillary sensors in microfluidic and point-of-care instrumentation," Sensors, vol. 10, 2010, pp. 3771–3797.

[31] www.vishay.com, Document Number: 53013, Revision: 25-Aug-09 39, pp. 39-39 [retrieved June 1, 2013].

[32] M. Borecki and M.L. Korwin-Pawlowski, "Optical capillary sensors for intelligent microfluidic sample classification," in "Nanosensors: Theory and Applications in Industry, Healthcare and Defence," T.C. Lim, Ed., CRC Press, Boca Raton, FL, USA, 2011, pp. 215–245.

[33] P. Rugeland, C. Sterner, and W. Margulis, "Visible light guidance in silica capillaries by antiresonant reflection," Optics Express, vol. 21, 2013, pp. 29217–29222.

[34] R.S. Romaniuk, "Geometry design in rerfractive capillary optical fibers," Photonics Letters of Poland, vol. 2, 2010, pp. 64–66.

[35] J. Gryglewicz, P. Firek, J. Jasiński, R. Mroczyński, and Jan Szmidt, "Characterization of thin Gd2O3 magnetron sputtered layers," Proc. of SPIE, vol. 8902, 2013, pp. 89022M.

[36] A.G. de Souza1, J.C. Oliveira Santos, M.M. Conceição, M.C. Dantas Silva, and S. Prasad, "A thermoanalytic and kinetic study of sunflower oil," Brazilian Journal of Chemical Engineering, vol. 21, 2004, pp. 265–273.